CONCENTRATION DEPENDENCE OF VISCOMETRIC PROPERTIES OF SHORT CHAIN POLYMER SOLUTIONS[1]

T. Kairn[2] , P. J. Daivis,[2,3], M. L. Matin[2] and I. K. Snook[2]

[1]Paper presented at the Fifteenth Symposium on Thermophysical Properties, June 22-27, 2003, Boulder, Colorado, U.S.A.

[2]Department of Applied Physics, RMIT University, GPO Box 2476V, Melbourne, Victoria 3001, Australia

[3]To whom correspondence should be addressed. E-mail: peter.daivis@rmit.edu.au

ABSTRACT

Relationships between polymer conformation, viscometric behaviour and concentration are observed and evaluated through a series of non-equilibrium molecular dynamics simulations of the behaviour of 20-site polymers in solution with explicit solvent across the full concentration range.

The zero-shear viscosities, first normal stress coefficients and steady-state shear compliance of the solutions are examined alongside conformational properties including the mean squared radius of gyration and the excluded volume effect.

These short chain polymers are observed to remain in an effectively dilute solution up to relatively high concentrations, before exhibiting both hydrodynamic and static screening. While the theories of Rouse and Zimm accurately describe the melt and dilute behaviours of this system, respectively, it is found that conformational data are not well described by the mean field or scaling theories.

KEY WORDS: bead rod model polymer; non-equilibrium molecular dynamics; polymer solution; shear flow; viscosity.

1 INTRODUCTION

This study examines the viscometric properties of short polymer chains in solution through a series of non-equilibrium molecular dynamics (NEMD) simulations. The viscometric and conformational properties of short-chain polymer solutions are of importance to a range of polymer science applications, including lubrication technology.

Simulation-based analyses of viscometric properties have been previously undertaken using a system containing a single polymer molecule, where "concentration" throughout the periodic system is determined according to the number of solvent molecules in the periodic box [1, 2, 3]. In this study, NEMD simulations are completed on systems of 100 to 500 chain molecules. The polymer molecules themselves have polymerisation degree $N = 20$, and are suspended in a solvent of single-site molecules, so that polymer concentration can be modified by altering the percentage of sites within the simulation box which are constrained to form chains. This system can be regarded as a simple model for any solution where the solvent consists of roughly spherical molecules which are approximately the same mass as the monomer units of the polymers suspended in them, provided that all molecules are non-polar and without specific interactions such as hydrogen bonding or charge interactions. For example, this system can be usefully regarded as representing a range of specific systems such as eicosane ($C_{20}H_{42}$) dissolved in methane (CH_4), polystyrene ($(CH_2CHC_6H_5)_{20}$) dissolved in styrene ($CH_2CHC_6H_5$) or PDMS ($(CH_3)_3SiO((CH_3)_2SiO)_{20}(CH_3)_2SiOH$) dissolved in TMS ($(CH_3)_4Si$), where each of these systems consist of polymer molecules constructed from 20 vaguely spherical units each, suspended in a solvent comprised of molecules very similar to the monomer unit of each polymer.

Since our simulations are performed at a range of very low homogeneous shear rates, the zero-shear-rate viscosity, η, can be easily identified for each concentration. Charting the changes in η as polymer concentration increases allows us to test the theories of chain behaviour.

The current authors are unaware of any other computational or experimental study which examines viscometric and conformational behaviour over the entire concentration range. The fragmentary nature of many experimental studies of viscosity and concentration mirrors the disjointedness of the relevant theory. Separate relations exist to describe viscosity behaviour in the dilute, semi-dilute and concentrated regimes. The aim of the current study is to examine the relationships between viscosity, conformation and concentration exhibited by a short-chain polymer solution, with reference to some of the various theoretical models available.

2 MOLECULAR MODEL AND SIMULATION TECHNIQUE

The simulation technique used to achieve the results contained herein has been reported previously [4]. Briefly, we use a non-equilibrium molecular dynamics (NEMD) code (described by Matin, Daivis and Todd [5]) which explicitly applies the molecular version of the SLLOD equations of motion to all particles

in the system, including those comprising the solvent and solves these equations at each time-step by a fourth order Gear predictor-corrector scheme. The solvent molecules are modeled as Lennard-Jones (LJ) spherical particles, while the polymer molecules are made up of 20-site chains of identical spheres. These chains are simulated according to a bead-rod model with truncated and shifted LJ (LJ) interactions between all beads ('sites') except those which are bonded to each other within a molecule. The LJ potential describing all interactions in the system is truncated and shifted so that potential has no discontinuity and is zero beyond a cutoff distance $r_c = 2^{1/6}\sigma$ (where σ is the distance at which the unshifted potential is zero). An LJ potential with this truncation point is often known as the WCA potential [6], and it results in purely repulsive interactions. This potential is convenient for computational work because it is short-ranged, and therefore computationally undemanding, but still retains the essential physics, i.e. the repulsive (excluded volume) interaction.

The molecular centre of mass temperature for the polymer chains (defined as proportional to the square of the centre of mass momentum of each chain divided by its molecular mass, per number of number of translational centre of mass degrees of freedom available to the molecules) is kept constant through the inclusion of a thermostatting term derived from Gauss' principle of least constraint. This algorithm, including the details of the constraint algorithm, has been discussed previously [7, 8, 9] and we refer the reader to previous work [10, 11, 12, 13] on the subtle but important issues involved in the application of homogeneous thermostats to flowing molecular fluids.

Bulk behaviour of this system simulated via periodic boundary conditions (PBCs) and the minimum image convention, which prescribes that the primary simulation box must be large enough so that each particle interacts only with the closest image of another particle [14]. Here, to allow for the homogeneous shear flow introduced to the system via the equations of motion, we apply Lagrangian rhomboid periodic boundary conditions, where periodic images are deformed in the x direction by an amount dependent on their location in the y direction. These effects result in a velocity gradient in the y-direction which, when the fluid state is at equilibrium and the flow rate is not too great [15], is equivalent to planar shear flow $\dot{\gamma} = \frac{\partial v_x}{\partial y}$. This method is periodic in space and time, allowing shear flow of an infinite bulk system to be simulated over very many time-steps.

The viscometric functions under consideration in this study are defined in terms of components of the pressure tensor P. The pressure tensor for the atomic fluid (single interaction site molecules) was calculated using the atomic pressure tensor, given by

$$\mathsf{P}_A V = \left\langle \sum_{i=1}^{N_a} \frac{\mathbf{p}_i \mathbf{p}_i}{M_i} - \frac{1}{2} \sum_{i=1}^{N_a} \sum_{j \neq i}^{N_a} \mathbf{r}_{ij} \mathbf{F}_{ij} \right\rangle, \tag{1}$$

while for the polymer solutions, it was calculated using the expression

$$\mathsf{P}_M V = \left\langle \sum_{i=1}^{N_m} \frac{\mathbf{p}_i \mathbf{p}_i}{M_i} - \frac{1}{2} \sum_{i=1}^{N_m} \sum_{\alpha=1}^{N} \sum_{j \neq i}^{N_m} \sum_{\beta=1}^{N} \mathbf{r}_{ij} \mathbf{F}_{i\alpha j\beta}^{inter} \right\rangle, \tag{2}$$

where $\mathbf{p}_i$ represents the total peculiar momentum of molecule i, as defined by the equations of motion, and $\mathbf{F}^{inter}_{i\alpha j\beta}$ represents the intermolecular force on site $i\alpha$ due to site $j\beta$. This means that the first term in each equation represents the kinetic component while the second describes the potential component of the pressure tensor.

For simple shear flow, η_s and Ψ_1 are useful material functions for representing and relating independent components of the stress tensor. η_s is the generalized non-Newtonian shear viscosity of a fluid subject to strain rate $\dot{\gamma}$ and is defined by:

$$\eta_s = -\frac{\mathsf{P}_{xy} + \mathsf{P}_{yx}}{2\dot{\gamma}}. \tag{3}$$

Ψ_1 is the first normal stress coefficient, given by the first two diagonal components of P,

$$\Psi_1 = \frac{\mathsf{P}_{yy} - \mathsf{P}_{xx}}{\dot{\gamma}^2} = \frac{N_1}{\dot{\gamma}^2}. \tag{4}$$

It is calculated from the first normal stress difference, N_1, which results directly from restoring forces acting in opposition to any flow-induced anisotropy in the fluid.

Steady-state values of η_s and Ψ_1 are linked by

$$\Psi_{1,0} = 2\eta^2 J_e^0. \tag{5}$$

where J_e^0 is the steady-state shear compliance of the fluid, which can also be calculated from η the steady-state viscosity of the solution, η_0 the solvent viscosity, S_2/S_1^2 the relaxation-time ratio and n_1 the polymer concentration, according to [16]

$$J_e^0 = \left(\frac{M}{n_1 RT}\right) \frac{(\eta - \eta_0)^2}{\eta^2} \frac{S_2}{S_1^2} \tag{6}$$

where R is the gas constant, M is the polymer molar mass and T is absolute temperature. This general relationship for polymer solutions can be applied to dilute solutions, where according to Zimm theory $S_2/S_1^2 = 0.206$. Alternately, in the high concentration limit, Rouse theory predicts that $S_2/S_1^2 = 0.400$.

These relationships have been shown to apply to simulations of a very short polymer chains, like those used here. For example, Matin [14] has shown that polymers with length $N = 20$ in a melt are flexible enough to exhibit a length-dependent viscosity consistent with Rouse theory. Furthermore, the applicability of the Zimm model to dilute solutions of short-chain polymers has been demonstrated by Dunweg and Kremer [17], down to $N = 30$. We are therefore confident that our short chains are accurately simulating real polymers, and that these theoretical relationships derived from polymer rheology should predict their behaviour.

3 RESULTS AND DISCUSSION

In the remainder of this paper, we express all quantities in terms of site reduced units for which the reduction parameters are the Lennard-Jones interaction

parameters ϵ and σ and the mass $m_{i\alpha}$ of site α on molecule i. These values are defined in terms of reduced temperature $T^* = \frac{k_B T}{\epsilon} = 1.0$, reduced density $\rho^* = \rho\sigma^3 = 0.84$ and the mass of each site $m^* = m_{i\alpha} = 1.0$, while time is scaled by $t^* = \sigma m^{\frac{1}{2}} \epsilon^{-\frac{1}{2}}$. For easy comparison of reduced and real quantities, relevant values for these variables are summarised in Table 1. The conversion to real units was completed by assuming that all sites in the solution could be regarded as modeling CH_4. Under this assumption, the system can be seen as representing a solution similar to eicosane dissolved in methane. The reliability of these straightforward conversions is limited by the fact that repeat unit of eicosane is CH_2 rather than CH_4, but the resulting values are useful in giving a general impression of the magnitudes of the parameters used in the simulation. The asterisk denoting reduced quantities will be dropped from here on.

Table 1: Values of simulation parameters and other quantities in real and reduced units. The approximate conversion to real units assumes that all sites are CH_4, with $m_{CH_4} = 2.66 \times 10^{-26} kg$, $\sigma = 3.817 \times 10^{-10} m$, $\epsilon = 2.0433 \times 10^{-21} J$ and $k_B = 1.3806 \times 10^{-23} JK^{-1}$.

Quantity	Reduced quantity	Value (reduced)	Value (real)
site mass	$m^* = m/m_{i\alpha}$	1	$2.66 \times 10^{-26} kg$
bond length	$d^* = d/\sigma$	1	$3.817 \times 10^{-10} m$
temperature	$T^* = \frac{kT}{\epsilon}$	1	$148K$
box volume	$V^* = \frac{V}{\sigma^3}$	11905	$6.620 \times 10^{-25} m^3$
number density	$\rho^* = \rho\sigma^3$	0.84	$1.510 \times 10^{28} sites/m^3$
mass density	$\rho_m^* = \rho\sigma^3/m_{i\alpha}$	0.84	$402 kg/m^3$
time-step	$t^* = \left(\frac{\epsilon}{m_{CH_4}\sigma^2}\right)^{\frac{1}{2}} t$	0.004	$5.53 fs$
strain rate $\dot{\gamma}$	$\dot{\gamma}^* = \left(\frac{\epsilon}{m_{CH_4}\sigma^2}\right)^{-\frac{1}{2}} \dot{\gamma}$	0.0022 (max.)	$1.60 \times 10^9 s^{-1}$
shear viscosity	$\eta_s^* = \left(\frac{\sigma^4}{m_{CH_4}\epsilon}\right)^{\frac{1}{2}} \eta_s$		
pressure	$p^* = \frac{p\sigma^3}{\epsilon}$		
energy	$E^* = \frac{E}{\epsilon}$		

The parameter n_1 defines polymer site fraction, the proportion of interaction sites in the system which belong to polymer molecules, and is used henceforward to describe the concentration of the systems. Table 2 lists the n_1 values used in this study and illustrates the relationship between this parameter and the mass density of polymer molecules in the solutions.

The shear rates used in these simulations were $\dot{\gamma}$ =0.0000, 0.0005, 0.00071, 0.0010, 0.0016 and 0.0022. MD simulations of polymer solutions usually use shear rates of between $\dot{\gamma} = 0.01$ and $\dot{\gamma} = 10$ (see, for example, Refs. [18] and [19]). The relatively low $\dot{\gamma}$ values used here fall within the range of shear rates accessible to current experiments [20].

The zero shear rate viscosity results shown in Table 2 were obtained via linear extrapolation to $\dot{\gamma}^2 = 0$ (using, in this case, a weighted least squares fit)

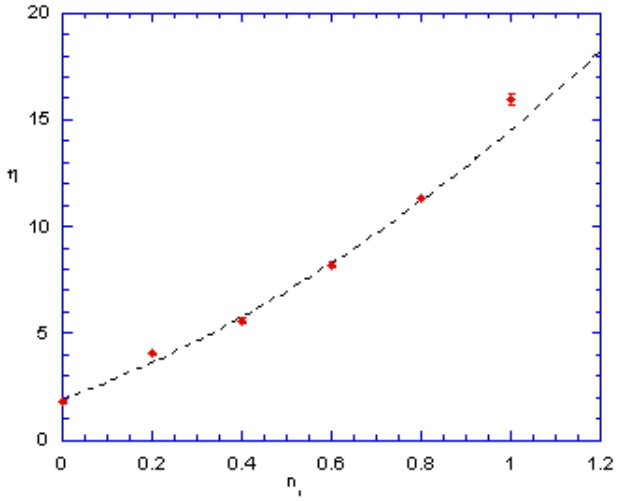

Figure 1: Zero shear viscosity, η, vs polymer concentration, n_1, showing second-order polynomial fit to all data points except $n_1 = 1.0$.

of our η_s vs $\dot{\gamma}^2$ data (illustrated in Ref [4]). It is evident from these results that zero shear rate viscosity (η) increases with increasing polymer concentration (n_1). This data is shown in Fig. 1, where it is fitted by a polynomial which obeys the Huggins equation,

$$\eta = \eta_0 \left(1 + [\eta]\, n_1 + k_H\, [\eta]^2 + ...\right) \tag{7}$$

where the Huggins constant k_H is 0.16 ± 0.4 and the intrinsic viscosity of the polymer n this very good solvent is $[\eta] = 4.0 \pm 0.4$. This relationship is expected to hold only for low concentration polymer solutions. However, our results show a persistence of dilute-like behaviour over a much broader concentration range.

Table 2: Simulation Parameters and Viscosity Data: Total number of sites (N_s), number of polymer molecules (N_m) and polymer site fraction (n_1) alongside zero shear rate first normal stress coefficient ($\Psi_{1,0}$), zero shear rate viscosity (η) and relaxation-time ratio (S_2/S_1^2) results.

N_s	N_m	n_1	$\Psi_{1,0} \times 10^{-2}$	η	S_2/S_1^2
10000	000	0.0	-0.3 ± 0.8	1.8 ± 0.1	
10000	100	0.2	-0.6 ± 0.4	4.03 ± 0.7	-0.06 ± 0.03
10000	200	0.4	5.5 ± 0.9	5.60 ± 0.9	0.38 ± 0.09
10000	300	0.6	7.8 ± 0.7	8.2 ± 0.1	0.28 ± 0.04
10000	400	0.8	15.0 ± 0.8	11.3 ± 0.1	0.33 ± 0.03
10000	500	1.0	33 ± 2	16.0 ± 0.3	0.45 ± 0.05

Our study of the conformation of this system [4] confirms this observation in that the polymer molecules in the system exhibit a strong excluded volume effect, up to a concentration greater than $n_1 = 0.4$. For higher concentrations this effect declines, but it is not until the $n_1 = 1.0$ melt is reached that the polymers in the system begin to display ideal Gaussian behaviour. The mean field theory predicts that polymer solutions will exhibit an increasing degree of excluded volume screening as polymer concentration is increased, with excluded volume interactions being fully screened in concentrated solutions, whereas the scaling theory predicts that full excluded volume screening and Gaussian behaviour should be seen at lower, semi-dilute concentrations [21]. Our results are easily reconciled with these theoretical predictions, in terms of both viscosity and conformation, if the system is regarded as persisting in an extended dilute state up to relatively high concentrations (greater than $n_1 = 0.4$), as a result of both the shortness of the polymers and the good quality of the Lennard-Jones solvent.

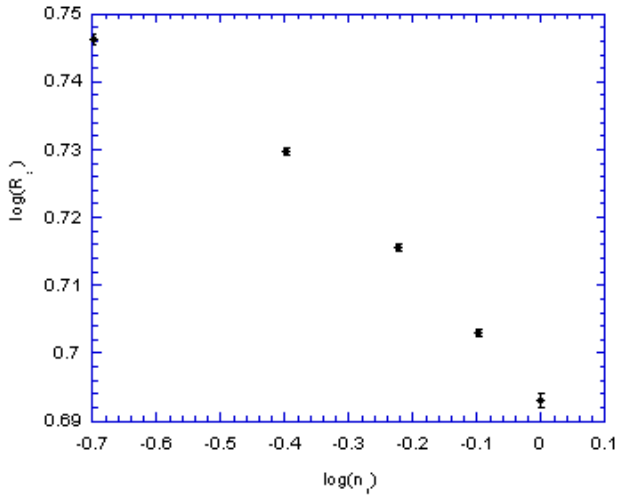

Figure 2: Logarithm of mean squared radius of gyration (R_g^2) vs logarithm of concentration ($log(n_1)$).

These observations sit uncomfortably alongside the results of our examination of the scaling behaviour of the mean squared radius of gyration (R_g^2), with concentration (see Fig. 2). Mean field theory predicts a scaling exponent of $-\frac{1}{2}$ between R_g^2 and n_1, whereas scaling theory predicts an exponent of $-\frac{1}{4}$. While there exist experimental studies of the conformational behaviour of long chain polymers which conform to both of these predictions [22], our simulation results

reveal a much more slight scaling relationship for our short polymers, varying from $-\frac{1}{20}$ to $-\frac{1}{10}$ as concentration increases. This disagreement conflicts with the theoretically compatible variation in the excluded volume effect, discussed above, and implies that there is some failing in the predominant polymer solution theories, when applied to short-chain molecules.

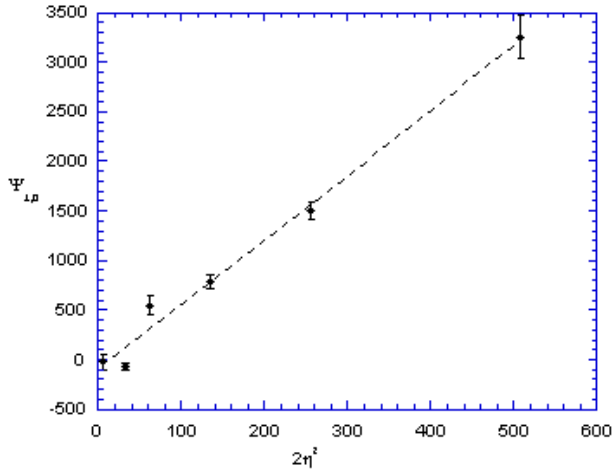

Figure 3: Limiting first normal stress tensor $\Psi_{0,1}$ vs $2\eta^2$. (Horizontal error bars are smaller than plot symbols.)

As a further exploration of the behaviour of this system, the limiting values of the first normal stress coefficient $\Psi_{1,0}$ are examined at each concentration. These values, listed in Table 2, are calculated as the gradients of weighted linear fits to the shear-dependent N_1 data (illustrated in Ref. [4]), which is linear over the low-shear region simulated. Fig. 3 shows the value of $\Psi_{1,0}$ at each concentration plotted against $2\eta^2$, a multiple of the zero shear viscosity of each solution. Relating equation 5 to this figure leads to the conclusion that the steady-state shear compliance of the fluid remains constant at $J_e^0 = \Psi_{1,0}/2\eta^2 = 6.8 \pm 0.3$ and does not appreciably vary with concentration.

This contrasts with the behaviour of J_{eR}^0, the reduced steady-state shear compliance, which is regarded as being equivalent to S_2/S_1^2, the relaxation-time ratio of the fluid. Combining equations 5 and 6 results in

$$J_{eR}^0 = \frac{\Psi_{1,0} n_1 RT}{2M\left(\eta - \eta_0\right)^2} = \frac{S_2}{S_1^2}. \tag{8}$$

Here the ratio of relaxation times, S_2/S_1^2, represents the degree of hydrodynamic interaction in the system. As noted in Section 2, Zimm theory predicts a value

of $S_2/S_1^2 = 0.206$ for low-concentration systems, whereas Rouse theory predicts that $S_2/S_1^2 = 0.400$, in the high concentration limit.

In Fig. 4, these values are plotted against $n_1\,[\eta]$, where they are expected to form a universal curve, independent of molecular weight. It is clear that, while the result for the $n_1 = 0.2$ system falls worryingly below the expected minimum of 0.206, S_2/S_1^2 values generally trend towards the Rouse prediction, for high concentrations.

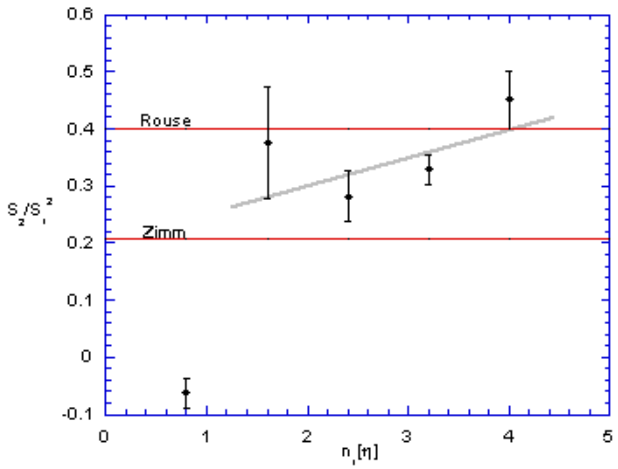

Figure 4: Ratio of relaxation times (S_2/S_1^2) vs concentration (n_1), showing Rouse ($S_2/S_1^2 = 0.400$) and Zimm ($S_2/S_1^2 = 0.206$) values.

The change from Zimm-like to Rouse-like behaviour with increasing polymer concentration signifies a transition from a hydrodynamically interacting regime to a concentrated regime with full hydrodynamic screening. Evidently, both hydrodynamic and static screening effects are apparent in the behaviour of this system.

4 CONCLUSION

By examining the behaviour of $N = 20$ CWA polymer chains solvated by a Lennard-Jones monatomic fluid, over the entire concentration range, we have shown that a system of very short polymers in the steady-state at low shear can exhibit significant deviation from the behaviour predicted by accepted theoretical approaches.

As polymer concentration is increased, the system examined here shows a clear trend from Zimm-like to Rouse-like behaviours, indicating that hydrody-

namic screening is increasing according to expectations. Similarly, an increase in static screening is apparent in the waning of the excluded volume effect observed at high concentrations. The behaviour of this static screening is predicted by the mean field and scaling theories, which regard this effect as the mechanism behind changes in polymer conformation and make consequent predictions for the scaling behaviour of R_g^2.

The fact that for these short-chain polymers, screening behaviours are observed while R_g^2 does not exhibit the expected scaling behaviour may indicate that static screening does not act as the mechanism for changes in polymer dimensions as current polymer theory suggests. Clearly, this analysis suggests the existence of a theoretical disparity worthy of further examination.

ACKNOWLEDGEMENTS

This work was supported by the Cooperative Research Centre for MicroTechnology and through an Expertise Grant from the Victorian Partnership for Advanced Computing. We would like to thank the CSIRO/Bureau of Meteorology High Performance Computing and Communications Centre and the Australian and Victorian Partnerships for Advanced Computing for generous allocations of computer time.

References

[1] C. Pierleoni, and J-P Ryckaert, *J. Chem. Phys.* **113**(2000).

[2] Y. N. Kaznessis, D. A. Hill, and E. J. Maginn, *J. Chem. Phys.* **109** (1998).

[3] I. Bahar, B. Badur, and P. Doruker, *J. Chem. Phys.* **99** (1993).

[4] T. Kairn, P. J. Daivis, M. L. Matin, and I. K. Snook, in preparation.

[5] M. L. Matin, P. J. Daivis, and B. D. Todd, *J. Chem. Phys.* **113** (2000). Erratum: M. L. Matin, P. J. Daivis, and B. D. Todd, *J. Chem. Phys.* (2001).

[6] J. D. Weeks, D. Chandler, and H. C. Andersen, *J. Chem. Phys.* **54** (1971).

[7] R. Edberg, D. J. Evans, and G. P. Morriss, *J. Chem. Phys.* **84** (1986).

[8] R. Edberg, G. P. Morriss, and D. J. Evans, *J. Chem. Phys.* **86** (1987).

[9] G. P. Morriss, and D. J. Evans, *Comput. Phys. Commun.* **62** (1991).

[10] K. P. Travis, P. J. Daivis, and D. J. Evans, *J. Chem. Phys.* **103** (1995).

[11] K. P. Travis, P. J. Daivis, and D. J. Evans, *J. Chem. Phys.* **103** (1995). Erratum: K. P. Travis, P. J. Daivis, and D. J. Evans, *J. Chem. Phys.* **105** (1996).

[12] K. P. Travis, and D. J. Evans. *Mol. Simulat.* **17** (1996).

[13] P. Padilla, and S. Toxvaerd. *J. Chem. Phys.* **104** (1996).

[14] M. L. Matin, *Molecular Simulation of Polymer Rheology* Ph. D. Thesis (Applied Physics, RMIT University, Melbourne, 2001).

[15] S. Hess, *Int. J. Thermophys.* **23** (2002).

[16] J. D. Ferry, *Viscoelastic Properties of Polymers* (John Wiley & Sons Inc., New York, 1980).

[17] B. Dunweg, and K. Kremer, *Phys. Rev. Lett.* **66** (1991).

[18] W. Brostow, and M. Drewniak, *J. Chem. Phys.* **105** (1996).

[19] S. Hess, C. Aust, L. Bennett, M. Kroeger, C. Pereira Borgmeyer, and T. Weider, *Physica A* **240** (1997).

[20] S. Bair, C. McCabe, and P. T. Cummings, *Phys. Rev. Lett.* **88** (2002).

[21] M. Doi, and S. F. Edwards, *The Theory of Polymer Dynamics* (Clarendon Press, Oxford, 1986).

[22] K. Adachi, Y. Imanishi, T. Shinkado, and T. Kotaka,*Macromolecules* **22** (1989).